Modeling Earthquake Seismology

Benjamin Harris
Physics Department, The College of Wooster, Wooster, Ohio 44691, USA
(Dated: May 10, 2013)

Earthquakes result from plate tectonic behavior just below Earth's crust. Seismology is the study of earthquake dynamics. We modeled earthquake seismology by studying stick-slip friction with three spring-block models. The first was a one-dimensional three block system, pulled by a driving motor. The second is a two-dimensional, nine block system pulled from the center. The third is a two-dimensional, nine block system pulled more evenly. Earthquakes follow a power law known as the Gutenberg-Richter law with a power of $n = -1$. Our three models seemed to tend toward behavior in accordance with the Gutenberg-Richter law. For our three systems, we measured powers of -1.0 ± 0.3, -0.7 ± 0.2, and -1.3 ± 0.2 respectively. With more data collection and a more significant number of events, it may be possible to show a more strong correlation to the power law behavior.

I. INTRODUCTION

Earthquakes are naturally occurring events in the Earth's lithosphere, resulting from plate tectonic activity. Earthquakes primarily occur at transform boundaries, subduction zones, and along mid ocean ridges. Strike-slip faults exist where two parallel tectonic plates are sliding past one other below the Earth's crust at a transform boundary. Subduction zones exist in the oceanic crust where one tectonic plate is wedging under another at a convergent plate boundary. Convergent boundaries occur in regions where tectonic plates are moving in opposite directions toward one other. Plate tectonic activity at mid ocean ridges is fairly constant, but slow. As the crust is weaker in these regions from the formation of new magma, not enough strain can build up to cause large magnitude events. Earthquakes at strike-slip faults and subduction zones can both have drastic consequences. Large transform boundaries may host devastative natural disasters along large strike-slip faults, two of the biggest being the San Andreas fault in California and the North Antatolian Fault in Turkey [3]. Large magnitude earthquakes in subduction zones can lead to tsunamis.

Strike-slip faults have primarily lateral movement, with roughly no vertical component [3]. Theoretically, strike-slip faults can transverse small areas or on a significant global scale [3]. Their ability to span around the globe comes from the fact that unlike convergent plate boundaries, their displacements are not limited by rock composition. Earthquakes at strike-slip faults occur relatively shallow in comparison to the earthquakes at subduction zones.

Earthquakes at subduction zones can occur at depths of a few hundred kilometers below the oceanic crust. While much plate tectonic activity in the oceanic crust goes unnoticed every day, earthquakes of great magnitudes can occur at subduction zones. These are known as megathrust earthquakes and can lead to the development of tsunamis, which can cause a lot of damage to coastal areas [1].

Given the destructive nature of earthquakes, we have learned to construct architecture in such a way that allows our buildings and people to be safer in areas at risk of damage due to plate tectonic activity. We are currently unable to predict earthquake's locations, magnitude, or timing, but hopefully through understanding the dynamics of the actual events, we will eventually be able to predict these events globally and account for them accordingly.

There is no complete laboratory or mathematical model for earthquakes, as they obey many complex behaviors on varying orders of magnitude [2]. Even if a full laboratory or mathematical model existed for earthquakes, it would have computational constraints [2]. Consequentially, laboratory and mathematical models with the goal of emulating earthquake behavior must focus on specific aspects of the quake. Stick-slip friction models are popular in modeling earthquakes. Some common laboratory models that show stick-slip friction are cellular automaton and spring-block models [4]. In spring-block models, earthquakes are viewed as a chain reaction of sliding blocks on some surface, controlled by the behavior of frictional forces working with elastic interactions [2].

Previously studied spring-block models include Burridge and Knopoff's work, in which they studied a one dimensional, eight block system driven by attaching the tops of the blocks by springs to a board and using the driving motor to move that board in order to examine the resulting behavior of the blocks [8]. Michael Davis built an analogous model using a one dimensional set up with four blocks and a pulley with hanging masses to apply a consistent force [6].

In this paper, we present the results of my study using three spring block models. One was created as a one-dimensional block system with three blocks. The two other spring-block systems consisted of nine blocks laid out two-dimensionally. In all cases, the blocks are attached by springs and moved along a wooden surface by a driving motor pulling string.

II. THEORY

Earthquake seismology is the study of earthquake dynamics. Earthquake seismology is modeled according to the Gutenberg-Richter power law. Stick-slip frictional systems are modeled as critical phenomena [5]. Criticality describes systems that follow scaling relations, fractal dimensions of behavior, and critical exponents [7]. In the case of earthquakes, criticality describes power law distributions [8]. As earthquakes occur due to millions of years of plate tectonic movement, they are used as the prototype for self-organized critical systems [5]. Per Bak discusses the nature of self-organized criticality, a term he coined, and its implication on large scales of evolution and economics in society [7]. Critical phenomena show up in many physical systems, but the concept of these systems being self-organized is debatable.

Systems studied in relation to the phenomenon of criticality reach critical states [7]. When our spring-block system approaches a critical state and any more energy is added via the driving motor, it approaches a super critical state. Following the transition, an event that moves all blocks in the system occurs. This is considered a large event and should occur much less frequently than small events. That particular relationship is analyzed as a power law. Critical phenomena in the context of seismology follow power law distributions. In the case of earthquakes, they obey the Gutenberg-Richter power law [8].

$$\log_{10} N = a - bM. \tag{1}$$

The Gutenberg-Richter power law expresses a relationship between the number of events N with the number of earthquakes of at least magnitude M within a given region. The slope $n = -1$ for the power law in earthquake seismology. The magnitude comes from the well known Richter scale for earthquakes [6]. The magnitudes of events on the Richter scale are based on the $\log_{10}$ of the energy dispersed in the event. The relationship of magnitude to energy is expressed as

$$M = \alpha + \beta \log_{10} E, \tag{2}$$

where β is a loosely fixed constant, but Richter uses the value of $\beta^{-1} = 1.5$ [8]. Combining Eqs. (1) and (2), the logarithmic relationship of the number of events to the seismic energy is expressed as

$$\log_{10} \frac{N}{N_0} = -b\beta \log_{10} E, \tag{3}$$

where E is the total seismic energy of an event, assumed to be proportional to the potential energy released [8]. For earthquakes measuring less than 7.1 on the Richter scale, $b = 0.58$ [8].

In the context of a spring-block system, that potential energy is released from the springs and the blocks stick-slip along the surface. Our spring-block model is likely a better representation of small magnitude events than it is of the largest, most destructive earthquakes [8]. In a spring-block model, we use at the potential energy released during the events as a comparison to earthquake magnitude. To find the potential energy U stored in the springs

$$U = \frac{1}{2} k x^2 \tag{4}$$

and assuming elasticity in accordance with Hooke's law, we can use

$$U = \frac{1}{2} k_1 (x_0 - x_{1,m} - l_1)^2 + \sum_{n=2}^{N} \frac{1}{2} k_1 (x_{n-1} - x_{n,m} - l_n)^2 \tag{5}$$

where k is the spring constant, l_n is the length of the corresponding spring, $x_{m,n}$ is the position in x of the center of the m^{th} block after the n^{th} event [8]. The spring constant, which correlates to its stiffness, is found with Hooke's law [3]

$$F = -kx. \tag{6}$$

Simplifying Eq. (3) and using potential U of the system, we get

$$\log_{10} \frac{N}{N_0} = -n \log_{10} U, \tag{7}$$

with slope n. In earthquakes, $n = -1$, which is the value that the spring-block models will be compared to.

III. PROCEDURE

The apparatus is a spring-block model prepared for three different experimental setups. The blocks used in the system are constructed of two smaller sanded plywood blocks, one on top of the other. Each of the smaller blocks was cut by hand with a panel saw and French saw. Each small block was cut in dimensions of approximately 10.1 cm long, 5.49 cm wide, and 1.2 cm thick. As such, the full blocks used in the system measured 10.1 cm long, 5.49 cm wide, and 2.4 cm thick. As all 18 smaller blocks used were cut by hand, they were not cut exactly the same, but they were close. The two blocks that comprise a larger block of the system are placed one on top of the other and attached with wood glue. We measured the full blocks of the system to have a mass of 77.52 g and an interacting surface area with the plane of 24.24 cm^2. Fig. 1 shows the whole block.

The blocks are connected to one other by compression springs with spring constants of 98 N/m and an unstretched length of 3.70 cm. The springs are connected to the blocks by squeezing the ends of them under a staple inserted into the sides of the wood that are pointed toward another block. As the plywood is too dense for the staple gun to fully insert the staples, we hammered

FIG. 1: One of the blocks used in the three experiments constructed of two smaller blocks, staples to hold the springs, and wood glue to keep the blocks together.

the staples in just enough to securely squeeze the ends of a spring under the staples, connecting two blocks to each other. The system was set up with either three or nine large blocks, depending on the trial.

The apparatus is designed to run the experiment in three manners. First, the experiment was run in one dimension with a single row of three blocks. In the second and third experiment, we account for two spatial dimensions of interaction by setting up the 3×3 block system. The difference between the second and third orientation is how force is applied to the system. In all three experiments, force is applied to drag the blocks across a flat, planar wooden surface by attaching a motor that spins a wheel. Twine is wrapped around the wheel attached to the axle spun by the motor.

In the first scenario, for the one dimensional case, the twine on the wheel is attached to the end of a spring on the central block closest to the motor. It allows for consistent application of force in one location and in one direction. Experiment 1 is the most simple of the three experiments and is being used compare results with previously conducted 1-D studies by Burridge and Knopoff [8], as well as Michael Davis [6]. The motor in figure 2 spins the wheel on the axle so that the string is pulled from under the wheel to avoid force being applied from above the system of springs and blocks. Fig. 2 shows the experimental set up for the first case.

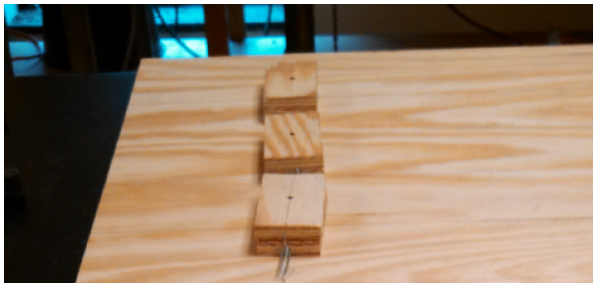

FIG. 2: The orientation of the system for experiment 1.

In the second experiment, for a two-dimensional case, the twine on the wheel is attached to the end of a spring on the central block closest to the motor. All nine blocks are pulled from this point, which is the same point as the 1-D case. The difference is the addition of blocks in the y-direction. The addition of blocks allows for more ways for the system to interact, but another spatial dimension of movement is not added, as the force is still applied in the x-direction. Fig. 3 shows the experimental set up for the second case.

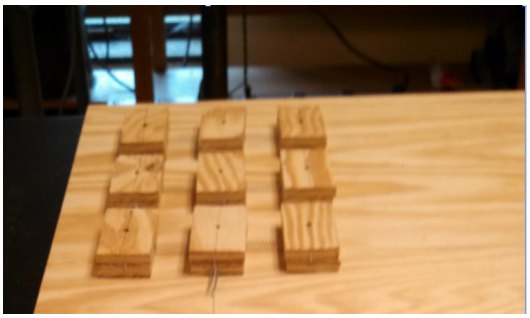

FIG. 3: The orientation of the system for experiment 2.

Due to the motor only pulling from one spot, the 3×3 spring-block system warps. The springs move in a way that we can't accurately measure the energy stored in them. Fig. 4 shows the arrangement that the spring-block model moves in with only central pull.

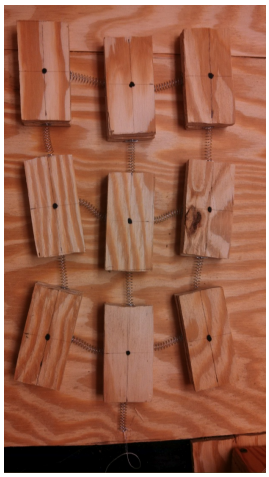

FIG. 4: The resulting configuration of blocks from a central pull in a nine block system that allows for two dimensions of interaction.

In the third experiment, our other two-dimensional case, we examine the properties of the system with an even pull across all blocks on the side of the motor, instead of all of the pull being from one spot. To allow for the even pull on the 3×3 model, we tied three strings, one from each of the three blocks on the side of the motor, between a vertically inserted staple to a wooden dowel rod. To apply force in the x-direction, string was tied

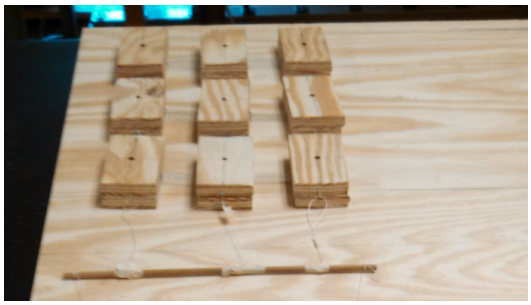

FIG. 5: The orientation of the system for experiment 3.

to the two ends of the dowel rod and glued for security. With the two points of attachment, the string was wrapped around the wheel of the motor in two layers and secured with masking tape to keep it from falling off of the track. Fig. 5 displays the experimental set up for the third experiment.

The base is made of the same sanded plywood as the blocks were cut from. The base is oriented so that the blocks move against the grain of the wood. The blocks, connected by springs, are placed on top of the base and tied to the motor in whichever fashion the trial demands. A camera is attached to a stand that positions it above the apparatus to video record the movement of the blocks as an event occurs. The top of all blocks have a black sharpie dot in the middle for ease of tracking. The motion of the blocks was tracked with Logger Pro, using video recordings of the three experimental set ups. Fig. 6 shows the spring-block system, driving motor, and camera used to collect data.

Data collection was conducted by using the camera situated above the apparatus. The camera was used to record video of the experiment, so that the movement of blocks could be tracked and analyzed in Logger Pro. As Logger Pro also requires that one provides a known scale, equidistant lines were drawn on the base every 10 cm for the program's ruler. Movement was tracked in the x and y dimensions, but the blocks in the system translated primarily in the x direction. Using the black sharpie dots centered on top of the blocks, we tracked the motion of each block in its respective trial for each frame of video recorded. The videos were recorded from the time that the motor was turned on until the blocks had been pulled as far as possible to remain on screen. The first experiments video had 560 frames to track for each of the three blocks and x_0. The second experiment with the force being applied from the center had 731 frames to track for each of the nine blocks, as well as x_0. The third experiment with the more evenly pulled force had 1128 frames to track for each of the nine blocks and x_0. Totaling the tracking of experiments 1-3, around 21,000 points were tracked. Position data for the blocks and connection to the string from the driving motor are the only data that were collected during the experiment.

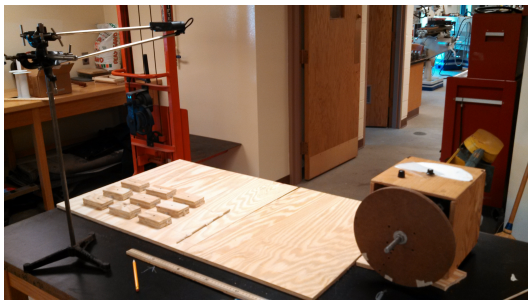

FIG. 6: The driving motor with the wheel spun on an axle is on the right side of the figure. The plywood base is placed on the table, with the combination of springs and blocks on top of it. The camera stand with the camera used to take data is on the left side.

IV. RESULTS & ANALYSIS

The goal of building a spring-block model to model earthquakes was to see if it obeys a power law distribution. Earthquakes obey the Gutenberg-Richter power law, which expresses a relationship between the frequency and magnitude of events in a given region. As the spring-block model is able to obey stick-slip behavior like earthquakes, we are testing to see if it follows the same power law relationship. We tested three different, but analogous experimental set ups described in the procedure. Fig. 7 displays an example of the data recorded in the three block, 1-D system.

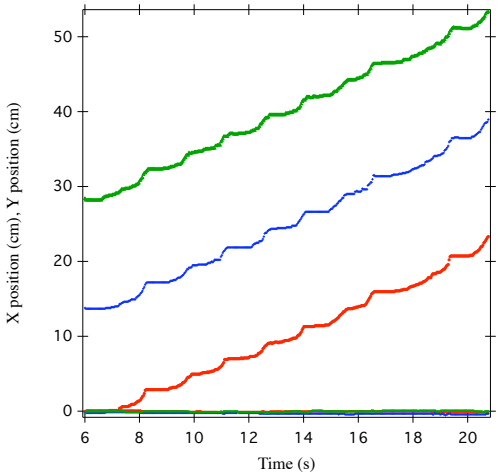

FIG. 7: The 1D spring-block data from Logger Pro. The red, blue, and green lines represent the movement in the x direction of the blocks over time. The bottom of the three (red) is the block furthest from the motor. Its center was used as the origin, which served as a reference point for the rest of the video analysis. The position data for the middle and closest block to the motor are the middle (blue) data set and the top (green) data set respectively. The bottom 3 lines represent movement in the y-direction for the three blocks.

FIG. 8: The block is pulled by a string attached to a spring. In this case with one block, x_0 is the location of the knot tied around the end of the spring.

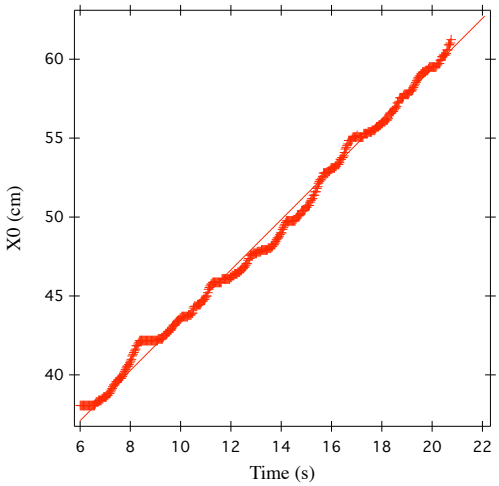

FIG. 9: In the plot, x_0 does not change constantly, but it is hard to track. To account for the challenge of tracking, x_0 is plotted against time and a linear fit is taken, giving an equation in the form of $y = mx + b$.

The position in x and y were tracked and plotted against time. As the force is only applied in the x-direction, the movement in the y direction is essentially nonexistent. Both two dimensional cases have nine blocks tracked instead of three, producing a similar, but more cluttered graph with the x and y coordinates being tracked.

Before analyzing the video of each spring-block system, we must first measure the spring constant k using Newton's second law $F = ma$ with Eq. (6). Each spring in the 1-D and 2-D systems is the same identical compression spring. Measuring the spring constant is simple experimentally, only requiring us to hang a mass from the spring and measure how long it stretches. By stretching the spring with a hanging mass, we measured the spring constant $k = 98\frac{\mathrm{N}}{\mathrm{m}}$.

The spring constant is essential in solving for potential energy U, as in Eq. (5). As spring-block models are assumed to have approximately constant velocity where the driving motor pulls the string x_0, we simplify the analysis by plotting the potential energy against x_0, which is proportional to time if the point does indeed move at a constant velocity [8]. Fig. 8 shows the connection point between the spring and the string, which is pulled by the motor.

Assuming the unchanging velocity for the point of contact between the driving motor and spring-block is convenient, as the potential energy stored in the springs is expressed as a function of the coordinates of the system and not the time [8]. Fig. 9 shows the fit for the one-dimensional case, but the same procedure is followed for all three experimental setups. The point of contact in experiment 2 is also the point at which the string wrapped around the wheel of the motor ties to the spring pulling the middle block on the side facing the motor. The point of contact for x_0 in experiment 3 is the middle of the dowel rod, which is pulled at both ends evenly by the driving motor.

Using a linear fit for each of the three experiments, we measured x_0 to change at 1.594 ± 0.005 cm/s, 1.395 ± 0.002 cm/s, and 0.861 ± 0.005 cm/s for experiments 1-3 respectively. Knowing the approximately constant velocity of the point of attachment, we used the summation in Eq. (5) to calculate the potential energy U. In the 1-D case, only three terms of x-movement contributed to the potential energy calculation. In the second experiment, the blocks warped very strangely. It is hard to get any analysis of the y contribution to changes in potential energy, but there was primarily movement in the x direction. As the stick-slip did not occur in the y direction, the potential energy was approximated with only the contribution from changes in x. In the third case with a more even pull on the system, potential energy was calculated with only the contribution from movement in x. The dowel rod allowed the system to not warp nearly as much as with the central pull, but when the potential energy was plotted in the y-direction, the changes were clearly minimal. Once again, the extra blocks spanning into the y-dimension provided more means for the system to interact, but there was still no driving force on the system in the y direction for y data to contribute much to changes in potential energy. Fig 10 shows the potential energy per block vs. the constantly changing x_0 for each of the three cases.

The first trial's potential energy graph looks more regular than the second or third trial's. This could be due to the motor pulling the one-dimensional spring-block model along the surface quickly in comparison to the two-dimensional spring-block models. As figure 10 shows the potential energy stored in the springs for each case, the drops show a release of potential energy, known as an event. These events are what models earthquake behavior, as the blocks stick and slip across the surface. To count events of varying magnitudes, we used Igor Pro to rotate the potential energy data and create a delta wave. The delta wave tracked the change in potential energy for each step in time. Positive values correspond to adding potential energy into the system by pulling on it with the driving motor. Negative values correspond to that potential energy being released by the springs, which is what is required for an event to occur. As we are looking at the relationship of events' magnitudes to their frequency. To do so, did not consider the data corresponding to energy

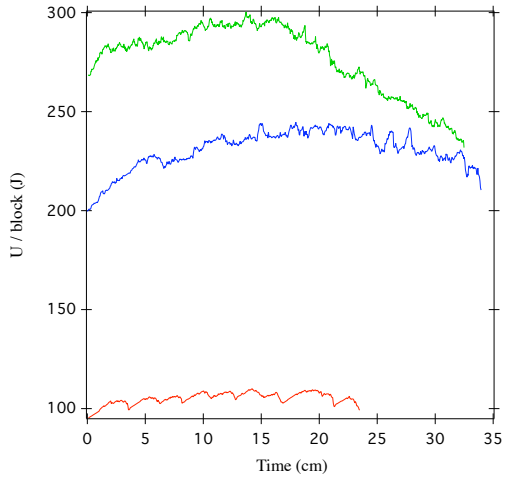

FIG. 10: The potential energy per block of the three experiments vs. the constantly changing x_0 approximated by linear fits of the x_0 data from Logger Pro analysis. The bottom red data is the potential energy per block of the one-dimensional system. The blue middle data represents the nine block system with central pull. The green represents the nine block model with an even pull.

being added into the system, but instead looked at the negative values, corresponding to the release of energy from the springs. Fig. 11 shows a curve of the events' magnitudes vs. their unit-less sequential number on the sorted list.

The 1-D case appears to have a step-like feature. It could be due to a couple factors involving Logger Pro.

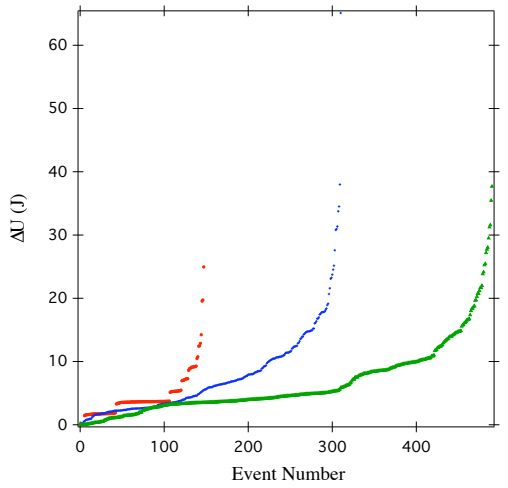

FIG. 11: The magnitude of events vs. the order on a list sorted low to high. All three experiments' data are shown here with experiment 1 as red circles, experiment 2 as blue plus signs, and experiment 3 as green triangles. The first experiment's data ends the soonest because it has the shortest video and smallest amount of events. The opposite is true for experiment 3.

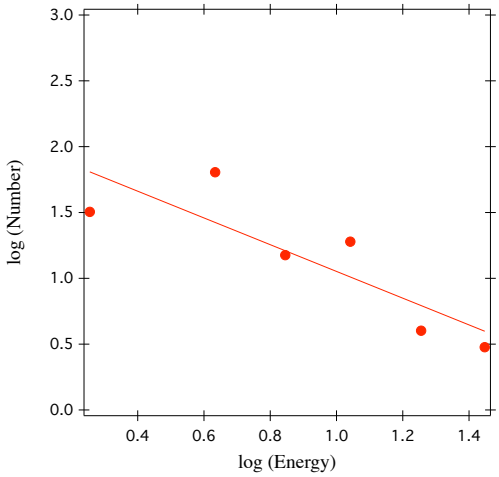

FIG. 12: The logarithm of the number of events N vs. the logarithm of the potential energy U for the one dimensional case with a slope of -1.0 ± 0.3.

One prospect is that, due to the difficulty in tracking the points, some intermediate movements were missed, possibly causing larger jumps in tracking throughout the video. Another possibility is that we simply don't have enough data points of events since this is a shorter run than the two-dimensional models, as the three blocks pulled across the surface quicker than the nine block systems. This could be fixed with more time to record video of the system and taking data with Logger Pro, but it is not believed to be a physical characteristic of stick-slip events.

The end goal of the analysis is to check whether or not the three spring-block systems correlate with the Gutenberg-Richter power law. To do so, we used a Igor Pro macro written by Dr. John Lindner in the College of Wooster Physics Department to count the number of occurences of events of various magnitudes. A problem in the analysis presented itself because certain bins must be set up to group the number of events in different ranges of magnitudes. We set up the bins of logarithmic ranges in four different ways, but it always cut data in half that was clearly close to the same magnitude. This might be an avoidable issue with more data for the three systems. When making a log-log plot of the number of events vs. the bins of the potential energy ranges of these events, Igor Pro ran into trouble. The issue came with taking a logarithm of zero, resulting in values of $-\infty$, which could not be plotted. Accounting for the lack of sufficient event data and the unnecessary splitting of the magnitudes by clumping together the events close to each other in potential energy change, the systems behave similarly to the Gutenberg-Richter law. Fig. 12 shows the log-log plot of the number of events vs. the bins of magnitudes for the first setup.

For the first trial with three blocks being tracked, we measured a slope of -1.0 ± 0.3, in comparison to the expected $n = -1$. There is a large error bar for the

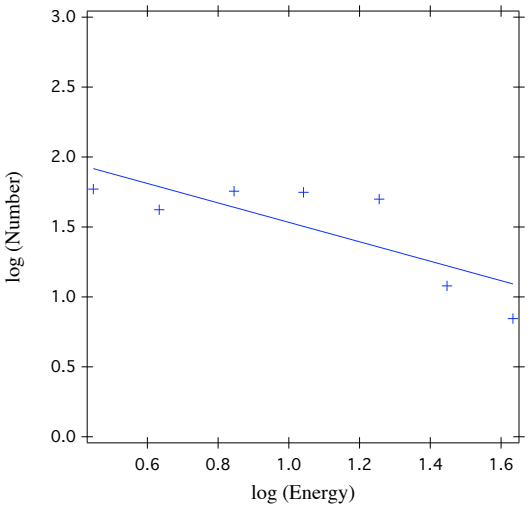

FIG. 13: The logarithm of the number of events N vs. the logarithm of the potential energy U for the 2D central-pull spring-block model with a slope of -0.7 ± 0.2.

relationship, but it is good evidence for the system to have been obeying stick-slip behavior in the same way that earthquakes do. Fig. 13 shows the log-log plot of the number of events vs. the magnitude of events for the second trial.

For the second trial, we measured a slope of -0.7 ± 0.2. This isn't quite the expected -1, but it is within the -0.5 to -1.5 range that earthquakes fall into depending on the area in which they occur [8]. The second experiment has some evidence to show its stick-slip behavior can be modeled similar to that of an earthquake. Fig. 14 shows the log-log plot of the number of events vs. the magnitude of events for the third trial with an even pull on the dowel rod.

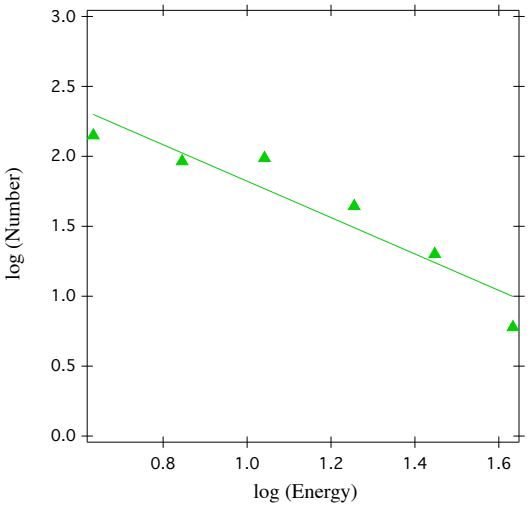

FIG. 14: The logarithm of the number of events N vs. the logarithm of the potential energy U for the third spring-block model with a slope of -1.3 ± 0.2.

Across the three separate experimental set ups, we measured the slopes of the log-log plots to be -1.0 ± 0.3, -0.7 ± 0.2, and -1.3 ± 0.2 for experiments 1-3 respectively, which are close to the expected $n = -1$. While the opportunity to take more data would be helpful, the three spring-block systems obey similar behavior to the Gutenberg-Richter law. A definitive statement of all three cases cannot be made without further analysis of the systems, but there is good evidence to support the laboratory models' usefulness in studying stick-slip friction in relation to earthquake seismology.

V. CONCLUSION

The spring-block model may be a suitable model for some aspects of earthquake dynamics. These three systems cannot definitively be said to model earthquake behavior before future work with them, but there is evidence to support that they are a reasonable representation of earthquake seismology. No spring-block system can fully represent an earthquakes behavior, as they are complicated systems which behave on many scales. We can indeed attain some insight from spring-block systems, however. The powers measured for the three different systems were measured to be -1.0 ± 0.3, -0.7 ± 0.2, and -1.3 ± 0.2 respectively, compared to the expected -1 from the Gutenberg-Richter power law.

Acknowledgments

I would like to thank Dr. Lehman for advising my Junior Independent Study Thesis, as well as Matthew Schmitthenner for his services as my lab teaching assistant. I would like to thank Dr. Lindner for writing the macro in Igor Pro necessary to conduct my analysis. I thank Ian Wilson and Samuel Mermall for their willingness to join me in the physics workshop so that I was able to obey all proper safety precautions. I would also like to give thanks to the College of Wooster Physics department for funding my research and providing the space in which to conduct it.

[1] Finn Løvholt, Sylfest Glimsdal, Carl B. Harbitz, Natalia Zamora, Farrokh Nadim, Pascal Peduzzi, Hy Dao, Helge Smebye, "Tsunami Hazard and Exposure on the Global Scale," *Earth-Science Reviews*, **110** 58-73 (2012).

[2] Florian Jansen and Stefan Hergarten, "Basic Properties of a Three-Dimensional Spring-Block Model with Long-Range Stress Transfer," *Physical Review E*, **73**, (026124) 1-8 (2006).

[3] Hank Fossen, *Structural Geology*, 3rd Ed. (Cambridge University Press, Cambridge, UK, 2011).

[4] Hans Jacob S. Feder and Jens Feder, "Self Organized Criticality in a Stick-Slip Process," *Physical Review Letters*, **66** (20), 2669-2672 (1991).

[5] Maria de Sousa Viera, Giovani L. Vasconcelos, and Sidney R. Nagel, "Dynamics of Spring-Block Models: Tuning to Criticality," *Physical Review E*, **47** (4), R2221-R2224 (1993).

[6] Michael Davis "The Spring-Block Model of Earthquakes," College of Wooster Junior Independent Study Thesis (Unpublished) (2006).

[7] Per Bak, *How Nature Works: The Science of Self-Organized Criticality*, (Copernicus Press, New York City, NY, 1996).

[8] R. Burridge and L. Knopoff, "Model and Theoretical Seismicity," *Bulletin of the Seismological Society of America*, **57** (3), 341-371 (1967).